On the geometry of ocean surface waves

Article *in* OCEANOLOGIA · June 2011

DOI: 10.5697/oc.53-2.521

1 author:

Stanislaw R. Massel

Institute of Oceanology of thePolish Academy of Sciences

48 PUBLICATIONS **1,342** CITATIONS

Papers

On the geometry of ocean surface waves

doi:10.5697/oc.53-2.521
OCEANOLOGIA, 53 (2), 2011.
pp. 521–548.

KEYWORDS
Ocean surface waves
Wave slopes
Frequency-directional spectra
Surface wave area

Stanisław R. Massel

Institute of Oceanology,
Polish Academy of Sciences,
Powstańców Warszawy 55, Sopot 81–712, Poland

Received 20 December 2010, revised 18 March 2011, accepted 19 April 2011.

Abstract

The factors influencing the atmosphere-ocean transfer of mass and momentum, as well as incipient wave breaking and the amount of energy dissipated due to breaking, are discussed in detail. In particular, the influence of directional spreading on the statistics of surface wave slopes and the area of the wind-roughened ocean surface is demonstrated. Theoretical analysis and comparison with the available experimental data show that unimodal directional spreading is not able to reproduce the observed ratio of the cross-wind/up-wind mean square slopes. Better agreement is achieved when bimodal directional spreading, consisting of two wrapped-Gaussian distributions, is applied. The bimodal form suggested by Ewans (1998) is used in the paper. Moreover, the formulae developed here show that the increase in the area due to surface waves is rather small for both regular and irregular waves.

1. Introduction

The energy coming from the atmosphere produces an aerodynamically rough ocean surface with very high, unsteady waves. The water motion due to surface waves is the most dynamic factor observed in the marine environment. Wind-induced waves are basically three-dimensional, and they exhibit some directional spreading against the wind direction (Massel 1996).

Studies of ocean surface waves can be roughly divided into a few groups. Apart from the theoretical works on wave mechanics and its modelling, the basic wave studies deal with the interaction of surface waves and engineering structures in deep and shallow waters as well as with the influence of surface waves on the interaction between atmosphere and oceans. This interaction basically includes the cross-surface fluxes of mass, momentum and moisture. In this paper we discuss another important factor of air-sea interaction, namely, the roughness of the ocean surface. It is quite obvious that the intensity of the air-sea interaction and the roughness of the atmosphere-ocean interface depends strongly on the state and geometry of the ocean surface.

There are two elements of the ocean surface that determine its roughness: the surface slopes and the increase in the area of the wind-roughened surface when compared with the area of calm ocean. The wave slope characteristics, in particular, play an important role in the estimation of incipient wave breaking and the amount of energy dissipated. The purpose of this paper is to discuss the influence of the frequency-directional spectrum of surface waves on the statistical characteristics of the surface wave slope and the area of the wind-roughened surface. In contrast to the spectral and statistical characteristics of surface wave elevations, studies of surface slopes are not so numerous, mostly because of the difficulty of experimentally measuring local slopes. New discoveries regarding the directional energy spreading of surface waves have only recently enlightened the study of surface wave slopes, providing some insight into the modelling of surface slope statistics.

The paper is organized as follows. Current experimental and theoretical results with respect to sea surface slopes are reviewed in section 2. Section 3 provides a presentation of modern frequency and directional spectra, while section 4 deals with the modelling of sea surface slopes and compares theoretical and experimental slope characteristics. In section 5 the impact of the intensity of the regular and irregular wave motion on the sea surface area is developed. Finally, section 6 gives the main conclusions.

2. Review of some experimental and theoretical results regarding surface wave slopes

2.1. The Cox & Munk experiment

Several techniques have been developed for measuring sea-surface wave slopes. In the pioneering work of Cox & Munk (1954), the statistics of the sun's glitter on the sea surface was interpreted in terms of the statistics of the slope distribution. Cox & Munk observed that the probability

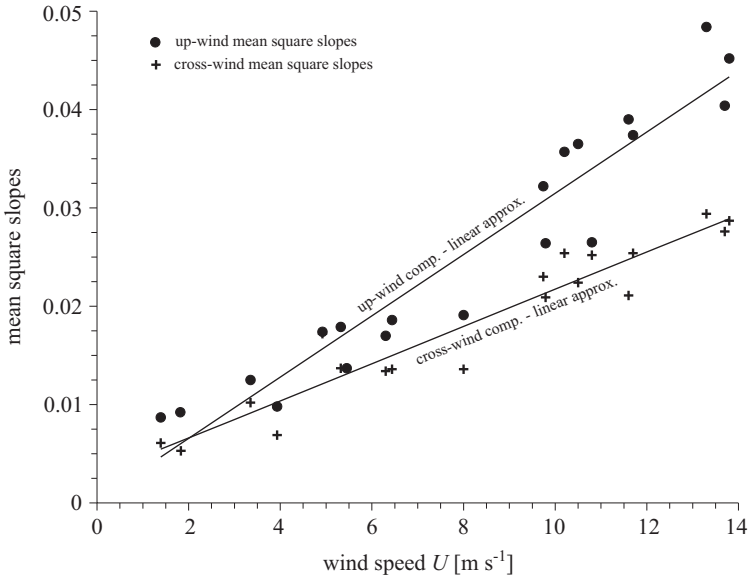

Figure 1. Experimental up-wind and cross-wind mean square slopes as a function of wind speed according to Cox & Munk (1954)

distribution of the cross-wind slope components are nearly Gaussian, whereas the distribution of the up-wind components of sea surface slopes can be approximated with some extra higher moments (in fact, they represent the Gram-Charlier distribution (Massel 1996)).

The resulting regression lines for the mean square slopes σ_u^2 and σ_c^2 demonstrate a nearly linear dependence on the wind speed U_{10} at the standard height of 10 m above the sea surface (see Figure 1):

$$\left.\begin{aligned} \sigma_u^2 &= 0.000 + 3.16 \times 10^{-3}\, U_{10} \\ \sigma_c^2 &= 0.0028 + 1.88 \times 10^{-3}\, U_{10} \end{aligned}\right\}. \tag{1}$$

Subscripts c and u refer to the cross-wind and up-wind directions respectively, and the coefficients 3.16 and 1.88 have the dimension [s m^{-1}].

The ratio of the mean square of the cross-wind and up-wind slope components varies between 0.54 and 1.0, with a mean value of 0.75. The authors found that the presence of oil slicks tends to suppress the shorter waves and reduce the mean square slope by a factor of 2 to 3.

2.2. The experiments of Pelevin & Burtsev (1975)

Pelevin & Burtsev (1957) published results of their experiment in the coastal region of the Black Sea. They confirmed Cox & Munk's nearly linear

dependence of the sea surface slope on the wind speed. For the mean square slopes they obtained

$$\left.\begin{aligned} \sigma_u^2 &= -0.0033 + 2.48 \times 10^{-3}\, U_{10} \\ \sigma_c^2 &= 0.00196 + 1.96 \times 10^{-3}\, U_{10} \end{aligned}\right\}. \tag{2}$$

The coefficients 2.48 and 1.96 have the dimension [s m^{-1}]. The wind speed and wind fetch during the experiment varied from 4 m s^{-1} to 7 m s^{-1}, and from 30 km to 100 km, respectively.

It is obvious that the observed sea surface slope depends on the intensity of the atmosphere-sea interaction. To include this phenomenon in the statistics of surface slopes, Woźniak (1996) introduced to the analysis the mean wave height $\bar{H}$ instead of the wind speed U_{10}. In particular, let us assume a very large wind fetch X. Thus, we obtain (Krylov et al. 1976)

$$\frac{g\bar{H}}{U_{10}^2} \approx 0.16 \tag{3}$$

and

$$U_{10}^2 = \frac{g}{0.16}\,\bar{H} \approx 61\,\bar{H}. \tag{4}$$

In fact, Woźniak used a slightly different relationship, based on the SMB method (Massel 1996), namely:

$$U_{10}^2 \approx 55.46\,\bar{H}. \tag{5}$$

2.3. The experiments of Hughes et al. (1977)

Hughes et al. (1977) combined optical, television and digital electronic techniques to design a fast response instrument for the measurement of sea surface slope. The data taken with the fully corrected, properly adjusted instrument from the Bute Inlet-George Strait indicate that the ratio of the mean square slopes σ_c^2/σ_u^2 varies from 0.50 to 0.80 for wind speeds from 4 to 8 m s^{-1}. No obvious trend in σ_c^2/σ_u^2 with wind speed has been observed. However, the third- and fourth-order moments in the Gram-Charlier probability distribution determined for nine data samples compared favourably with the earlier measurements by Cox & Munk (1954).

2.4. The influence of meteorological conditions on sea surface slopes

Observed surface wave spectra include a large variety of wavelengths, from very short capillary waves to long swell. The very short waves are

usually superimposed on the long waves, which form a background for them. Hwang & Shemdin (1988) examined the influence of the presence of a long ocean swell and unstable stratification at the air-sea interface on the sea surface roughness. The data from their TOWARD experiment showed that the mean square slope increases gradually with wind friction velocity u_* at low winds, followed by rapid growth near $u_* = 20$ cm s^{-1} and beyond, which resulted in mean square slopes much higher than those reported by Cox & Munk. According to Hwang & Shemdin, the swell is the primary factor that modifies this relationship.

Usually, the wind-generated sea is characterized by the wave age C_p/U_{10} (C_p is the phase speed of the peak component); when $C_p/U_{10} > 1$, swell conditions predominate. The measurements of surface slopes during the TOWARD experiment indicate that the presence of swell can either enhance or reduce surface roughness: in particular, for a low wind speed, when $C/U_{10} > 3$, there was a reduction in the mean square slope of up to 40%.

Another possible primary factor influencing the mean square slope is the atmospheric stability, which is generally expressed in terms of the Monin-Obukhov parameter:

$$\frac{z}{L} = \frac{g\kappa z\,\overline{w'T'_a}}{u_*^3 \bar{T}_a}, \tag{6}$$

where L is the Monin-Obukhov length scale, $\kappa \approx 0.4$ is the von Kármán constant, w' is the fluctuation component of the vertical velocity, z is the elevation above sea level, T'_a is the fluctuation in air temperature, and $\bar{T}_a$ is the mean air temperature. Hwang & Shemdin's (1988) data showed a reduction of the mean square slope for stable conditions (when $z/L > 0$). This reduction is nearly linear for mildly stable conditions with some limit at $z/L \approx 0.2$. Beyond this value, the slope does not decrease any more.

It should be noted that the direction of the slope vector deviates from that of the wind due to the presence of long waves. The steering of short waves away from the wind direction by long waves depends on the wave age, such that the greater the wave age, the more effective the steering.

3. Frequency and directional wave spectra

3.1. Definition of the frequency spectra

Up till now sea surface slopes have been discussed without any relation to the form of the frequency spectrum $S(\omega)$ (ω is the frequency) and directional spreading $D(\theta)$ (θ is the angle of wave propagation against the wind direction). Sea surface waves are fully described by the two-dimensional

frequency-direction spectrum $S_1(\omega,\theta)$, usually given as the product of the frequency spectrum $S(\omega)$ and the directional spreading $D(\theta,\omega)$:

$$S_1(\omega,\theta) = S(\omega)D(\theta,\omega). \tag{7}$$

Waves longer than the peak wavelength make only a very small contribution to the surface slope, and the influence of high frequency wave components on the statistics of sea surface slopes is substantial. In the classical JONSWAP spectrum (Massel 1996), the high-frequency tail is represented in the form of a ω^{-5} dependence. There are many other representations for this frequency region, which results in different estimates of the wave slope statistics (see, for example, Bjerkas & Riedel 1979, Apel 1994, Hwang & Wang 2001). In order to reduce these discrepancies, Elfouhaily et al. (1997) proposed a two-dimensional wave number spectrum valid over all wave numbers k and supplemented by the directional spreading function in the form

$$\Psi(k,\theta) = \frac{1}{2\pi}\, k^{-4}[B_l + B_h][1 + \Delta(k)\cos(2\theta)], \tag{8}$$

where B_l and B_h are the long-wave and short-wave curvature spectra respectively. It should be noted that such spectra are particularly useful for the radiometric remote sensing of the sea surface (see, for example, Heron et al. 2006).

Another representation of the high frequency spectra was put forward by Hwang & Wang (2001), who for the equilibrium and saturation parts of the wave number spectra assumed that

$$S_1(\omega) = \begin{cases} 2bg\, u_*\, \omega^{-4} & \text{for} \quad \omega_p < \omega \le \omega_i \\ Bg^2\, \omega^{-5} & \text{for} \quad \omega_i < \omega < \omega_u \end{cases}, \tag{9}$$

where $\omega_i = 6\omega_p$, and the friction velocity u_* is given by (Massel 2007)

$$u_* = \sqrt{C_z}\, U_{10}, \tag{10}$$

where

$$C_z \approx (0.8 + 0.065\, U_{10}) \times 10^{-3}. \tag{11}$$

The upper limit of the frequency ω_u above which wave components are suppressed by a slick is $\omega_u = \sqrt{gk_u} = \sqrt{2\pi g/0.3} \sim 14.33$ rad s^{-1}.

The impact of the low-frequency part of the spectrum on surface wave slopes is generally small, but for simplicity we will apply here the JONSWAP and Pierson-Moskowitz spectra (Hasselmann et al. 1973, Massel 1996),

when the high frequency part of the spectra attenuates according to the function $\approx \omega^{-5}$. Thus, we have:

$$S(\omega) = \alpha g^2 \omega^{-5} \exp\left[-\frac{5}{4}\left(\frac{\omega}{\omega_p}\right)^{-4}\right] \gamma^{\delta_1}, \tag{12}$$

in which $\gamma = 3.3$;

$$\delta_1 = \exp\left[-\frac{(\omega-\omega_p)^2}{2\sigma_0^2\,\omega_p^2}\right], \tag{13}$$

$$\sigma_0 = \begin{cases} 0.07 & \text{for} \quad \dfrac{\omega}{\omega_p} < 1 \\ 0.09 & \text{for} \quad \dfrac{\omega}{\omega_p} \geq 1 \end{cases}. \tag{14}$$

The coefficient α and peak frequency ω_p are defined by the non-dimensional fetch as

$$\alpha = 0.076\left(\frac{gX}{U_{10}^2}\right)^{-0.22}, \tag{15}$$

$$\omega_p = 7\pi\,\frac{g}{U_{10}}\left(\frac{gX}{U^2}\right)^{-0.33}. \tag{16}$$

When the peak enhancement factor $\gamma = 1$, the JONSWAP spectrum reduces to the Pierson-Moskowitz spectrum.

In the Pierson-Moskowitz and JONSWAP spectra, negligible energy is contained in the frequency band $0 < \hat{\omega} = \omega/\omega_p < 0.5$. Hence, we set the lower limit at $\hat{\omega}_l = 0.5$. The upper limit $\hat{\omega}_u$, which is not necessarily equal to ∞, requires more attention as its influence on spectral moments, especially on higher moments, is substantial. In particular, for moment m_n we have

$$m_n = \alpha g^2 \omega_p^{n-4} \int_{\hat{\omega}_l}^{\hat{\omega}_u} \hat{\omega}^{n-5} \exp\left(-\frac{5}{4}\hat{\omega}^{-4}\right) \gamma^r\, d\hat{\omega}, \qquad \hat{\omega} = \frac{\omega}{\omega_p}. \tag{17}$$

Let us now assume that $\hat{\omega}_l = 0$, $\hat{\omega}_u = \infty$, and $\gamma = 1$ in the Pierson-Moskowitz spectrum. Hence, the moment m_n becomes (Massel 2007)

$$\begin{aligned} m_n &= \alpha g^2 \omega_p^{n-4} \int_0^{\infty} \hat{\omega}^{n-5} \exp\left(-\frac{5}{4}\hat{\omega}^{-4}\right) d\hat{\omega} \\ &= \frac{\beta g^2 \omega_p^{n-4}}{4}\left(\frac{5}{4}\right)^{\frac{n-4}{4}} \Gamma\left(\frac{4-n}{4}\right), \end{aligned} \tag{18}$$

where $\Gamma(x)$ is the gamma function (Abramowitz & Stegun 1975). Equation (18) indicates that the fourth moment m_4, for example, becomes infinite as $\Gamma(0) = \infty$. The only way to calculate this moment for practical applications is to impose some threshold frequency $\hat{\omega}_u \neq \infty$. In oceanological and engineering practice it has usually been assumed that $\hat{\omega}_u = 6$. Waves with frequency $\omega = 6\,\omega_p$ can still be considered gravity waves, as the viscous effects are negligible. Therefore, using eq. (17), the moment m_4 for the JONSWAP and Pierson-Moskowitz spectra becomes (Massel 2007)

$$m_4 = 0.076\, a_4\, g^2 \left(\frac{gX}{U^2}\right)^{-0.22}, \tag{19}$$

where X is the wind fetch, V_{10} is the wind speed at the standard height of 10 m above sea level. The coefficient a_4 for the JONSWAP spectrum is $a_4 = 1.7057$, while for the Pierson-Moskowitz spectrum we have $a_4 = 1.5919$.

3.2. Directional spreading functions $D(\theta, \omega)$

Intuitively, wind waves propagate mainly in the wind direction and decrease monotonically with increasing angle θ. The first representations, still widely used for ocean wave models and engineering applications, are based on unimodal directional distributions. In particular, Longuet-Higgins et al. (1961), using field observations, proposed $D(\theta, \omega)$ in the form

$$D(\theta) = \frac{\Gamma(s+1)}{2\sqrt{\pi}\,\Gamma\left(s+\frac{1}{2}\right)} \cos^{2s}\left(\frac{\theta}{2}\right) \quad \text{for} \quad -\pi < \theta \leq \pi, \tag{20}$$

where s is the directionality parameter and $\Gamma(x)$ is the gamma function (Abramowitz & Stegun 1975).

It should be noted that this function does not depend on the frequency of the wave components. However, field studies by Mitsuyasu et al. (1975), Krylov et al. (1976), Hasselmann et al. (1980) and Donelan et al. (1985) indicate that unimodal directional distributions depend on the wave frequency and that the distributions are narrowest at the peak frequency and broader towards both higher and lower frequencies. In particular, the Mitsuyasu distribution takes the form (Massel 1996):

$$D(\theta, \omega) = A(s)\, \cos^{2s}\left(\frac{\theta - \theta_1}{2}\right), \tag{21}$$

where θ_1 is the mean wave direction and $A(s)$ is the normalization factor to ensure that

$$\int_0^{2\pi} D(\theta, \omega)\, d\theta = 1. \tag{22}$$

The frequency dependence is expressed by the following directionality parameter s:

$$s = \begin{cases} s_p \left(\dfrac{\omega}{\omega_p}\right)^{5} & \text{for} \quad \omega < \omega_p \\ s_p \left(\dfrac{\omega}{\omega_p}\right)^{-2.5} & \text{for} \quad \omega \geq \omega_p \end{cases}, \tag{23}$$

where s_p is the value of s at the peak frequency ω_p:

$$s_p = 11.5 \left(\frac{U}{C_p}\right)^{-2.5}. \tag{24}$$

The representation of Hasselmann et al. (1980) is based on data collected with a heave-pitch-roll buoy located 55 km off the Island of Sylt in the North Sea. It is valid for wind speeds from 6.8 to 15 m s^{-1} and for significant wave heights from 0.55 to 1.88 m. It takes the same form as the Mitsuyasu representation (eq. (21)), but with a slightly different dependence of parameter s on the non-dimensional frequency.

Donelan et al. (1985) proposed the directional spreading $D(\theta, \omega)$ in the form of the sech function as follows:

$$D(\theta, \omega) = 0.5\beta \operatorname{sech}^2 [\beta(\theta - \theta_1)], \tag{25}$$

where

$$\beta = \begin{cases} 2.61 \left(\dfrac{\omega}{\omega_p}\right)^{1.3} & \text{for} \quad 0.56 < \dfrac{\omega}{\omega_p} < 0.95 \\ 2.28 \left(\dfrac{\omega}{\omega_p}\right)^{-1.3} & \text{for} \quad 0.95 < \dfrac{\omega}{\omega_p} < 1.6 \\ 1.24 & \text{for} \quad \dfrac{\omega}{\omega_p} > 1.6 \end{cases}. \tag{26}$$

Banner's (1990) analysis of high-frequency stereo photographs showed that parameter β is not in fact constant at values of $\omega/\omega_p > 1.6$.

Ewans (1998) reported the results of measurements of wave directionality for fetch-limited sea states at Maui off the west coast of New Zealand. Using a heave-pitch-roll buoy, he showed that the integrated properties of the estimated angular spreading distribution are in general agreement with those observed in previous studies. However, the angular distribution becomes bimodal at frequencies greater than the spectral peak frequency. To describe this distribution, Ewans assumed that directional spreading is symmetrical about the mean wave direction, and each of the two components

have the wrapped-around Gaussian form (Mardia 1972, Massel 1996), with the same amplitude and the same angular spreading:

$$D(\theta,\omega) = \frac{1}{\sqrt{8\pi}\,\sigma(\omega)} \sum_{k=-\infty}^{k=\infty} \left\{ \exp\left[-\frac{1}{2}\left(\frac{\theta - \theta_{m_1}(\omega) - 2\pi k}{\sigma_\theta(\omega)} \right)^2 \right] + \right. \\ \left. + \exp\left[-\frac{1}{2}\left(\frac{\theta - \theta_{m_2}(\omega) - 2\pi k}{\sigma_\theta(\omega)} \right)^2 \right] \right\}, \tag{27}$$

where $\sigma_\theta(\omega)$ is the angular spreading of each frequency component, and θ_{m_1} and θ_{m_2} are the locations of the peaks such that $\theta_{m_1} = -\theta_{m_2}$. The locations of the peaks and the angular spreading are the following functions of the frequency ω:

$$\theta_{m_1}(\omega) = \begin{cases} 7.50 & \text{for} \quad \omega < \omega_p \\ \dfrac{1}{2}\exp\left[5.453 - 2.75\left(\dfrac{\omega}{\omega_p} \right)^{-1} \right] & \text{for} \quad \omega \geq \omega_p \end{cases} \tag{28}$$

and

$$\sigma_\theta(\omega) = \begin{cases} 11.38 + 5.357\left(\dfrac{\omega}{\omega_p} \right)^{-7.929} & \text{for} \quad \omega < \omega_p \\ 32.13 - 15.39\left(\dfrac{\omega}{\omega_p} \right)^{-2} & \text{for} \quad \omega \geq \omega_p \end{cases} . \tag{29}$$

Ewans & van der Vlugt (1999) discovered that the bimodality of the directional spectrum is also visible for the wave conditions occurring during tropical cyclones. Such sea states consist largely of a cyclone-generated swell component and a local wind sea. Following Kuik et al. (1988), they defined the so-called unimodal/bimodal parameter, which is a function of the skewness and kurtosis of the directional distribution. Using the data from the wave buoy deployed south-west of the North Rankin A platform, approximately 123 km off the north-west coast of Australia, they found that the bimodal directional distribution is associated particularly with the more energetic sea states prevailing during tropical cyclones. When the significant wave height is below 2 m, the contribution of the bimodal sea states to the total variance is somewhat less than 60 percent. In the region of the peak frequency of the spectrum, the components are generally unimodal, and the number of bimodal distributions increases at frequencies both above and below the peak frequencies.

A similar directional spreading was observed by Young et al. (1995) during experiments on Lake George, Australia. The lake has a depth

of 2 m, and the reported waves were in the range $1.7 < U_{10}/C_p < 3$. Directional spreading was narrowest in the region of the spectral peak ω_p and broadened at frequencies both higher and lower than ω_p. At frequencies of approximately $\omega > 2\omega_p$, the spreading function develops into a bimodal form. The existence of the bimodal directional form was supported by Banner & Young's (1994) theoretical analysis, in which the full solution of the non-linear spectral energy balance equation indicates that directional spreading in the high frequency region is controlled by the non-linear spectral transfer of energy through wave-wave interactions.

Note that Ewans' (1998) results showed no dependence of the bimodal distribution parameters on wave age. This means that the bimodal directional distribution is an invariant property of the wind-generated wave field. Wang & Hwang (2001) supported this conclusion, stating that directional biomodality is a very robust feature also occurring in waves generated by an unsteady wind in both deep and shallow waters, and that the frequency parameters of the bimodal directional distribution are invariant with respect to wave age during the transient wave growth period.

The form of the directional distribution $D(\theta, \omega)$ strongly influences the probability distribution of the wave surface slope and frequently discussed mean square slopes. In particular, the experiments discussed above showed that the average ratio between the cross-wind and up-wind mean square slope components varies from 0.75 to 1.03 on slick-covered ocean surfaces. Such a large value of the cross-wind slope component cannot be explained satisfactorily with the unimodal directional distribution, and better agreement is obtained when, for wave components shorter than the dominant wavelength, the bimodality of directional spreading is taken into account (Hwang & Wang 2001). In particular, the ATM data (airborne topographic mapper) of the 3D surface topography and bimodal directional function showed that the average ratio between cross-wind and up-wind slope components can reach a value of 0.88 ± 1.0.

4. Slopes of the ocean surface waves

4.1. Governing equations and definitions

In this section we will follow mainly the ideas developed by Massel (2007). Thus, let us define ε as a module of the local surface slope in the direction θ_1 against the x axis. For two slope components along the x and y axes we have

$$\varepsilon_x = \frac{\partial \zeta}{\partial x} = \varepsilon \cos\theta_1, \quad \varepsilon_y = \frac{\partial \zeta}{\partial y} = \varepsilon \sin\theta_1, \tag{30}$$

in which angle θ_1 increases anticlockwise from the x axis. We assume that the x axis is the wind direction. Therefore, the up- and cross-wind of waves surface slopes are $\varepsilon_u = \varepsilon_x$ and $\varepsilon_c = \varepsilon_y$ respectively.

To determine the statistical characteristics of wave slopes, we express the two-dimensional probability density function $f(\varepsilon, \theta_1)$ for the module slope ε and direction θ_1 in the form suggested by Longuet-Higgins (1957):

$$f(\varepsilon, \theta_1) = \frac{\varepsilon}{2\pi\sqrt{\Delta}} \times \\ \times \exp\left\{-\frac{\varepsilon^2(\sigma_y^2 \cos^2\theta_1 - 2\sigma_{xy}^2 \sin\theta_1 \cos\theta_1 + \sigma_x^2 \sin^2\theta_1)}{2\Delta}\right\}, \tag{31}$$

in which the corresponding mean square slopes are

$$\sigma_x^2 = \overline{\left(\frac{\partial\zeta}{\partial x}\right)^2}, \quad \sigma_y^2 = \overline{\left(\frac{\partial\zeta}{\partial y}\right)^2}, \quad \sigma_{xy}^2 = \overline{\frac{\partial\zeta}{\partial x}\frac{\partial\zeta}{\partial y}} \tag{32}$$

and

$$\Delta = \begin{vmatrix} \sigma_x^2 & \sigma_{xy}^2 \\ \sigma_{xy}^2 & \sigma_y^2 \end{vmatrix}. \tag{33}$$

The bar symbolizes the statistical averaging for a given time series of slopes.

For the x axis, parallel to the main wave direction, the mean square slope $\sigma_{\zeta_{xy}}^2$ is equal to zero, and eq. (31) becomes

$$f(\varepsilon, \theta_1) = \frac{\varepsilon}{2\pi\sqrt{\Delta}} \exp\left\{-\frac{\varepsilon^2(\sigma_c^2 \cos^2\theta_1 + \sigma_u^2 \sin^2\theta_1)}{2\Delta}\right\}, \tag{34}$$

with $\Delta = \sigma_u^2\sigma_c^2$. The subscripts c and u refer to the cross-wind and up-wind components respectively.

In order to compare the theoretical distribution of slopes with the Cox & Munk (1954) experiment, we rewrite eq. (24) as a function of two slope components ε_u and ε_c, i.e.

$$f(\varepsilon_u, \varepsilon_c) = f(\varepsilon, \theta_1) \cdot J = f(\varepsilon, \theta_1) \begin{vmatrix} \dfrac{\partial\varepsilon}{\partial\varepsilon_u}, & \dfrac{\partial\varepsilon}{\partial\varepsilon_c} \\ \dfrac{\partial\theta_1}{\partial\varepsilon_u}, & \dfrac{\partial\theta_1}{\partial\varepsilon_c} \end{vmatrix}. \tag{35}$$

Using the fact that

$$\varepsilon = \sqrt{\varepsilon_u^2 + \varepsilon_c^2} \quad \text{and} \quad \theta_1 = \arctan\left(\frac{\varepsilon_c}{\varepsilon_u}\right), \tag{36}$$

we obtain

$$J = \frac{1}{\sqrt{\varepsilon_u^2 + \varepsilon_c^2}}. \tag{37}$$

Substituting the above expression in eq. (35) yields

$$f(\xi, \eta) = \frac{1}{2\pi\sigma_u\,\sigma_c}\,\exp\left[-\frac{1}{2}\left(\xi^2 + \eta^2\right)\right], \tag{38}$$

where

$$\xi = \frac{\varepsilon_u}{\sigma_u}, \quad \eta = \frac{\varepsilon_c}{\sigma_c}. \tag{39}$$

Equation (38) takes the form of a two-dimensional Gaussian distribution. It should be noted that Cox & Munk (1954) used the two-dimensional, slightly modified Gaussian distribution (the so-called Gram-Charlier distribution) to fit their experimental data. The Gram-Charlier distribution takes the general form (Massel 1996)

$$f = [\text{Gaussian distribution}] \times \left[1 + \sum_{i,j} c_{ij}\, H_i\, H_j\right], \tag{40}$$

in which $H_i(x)$ are Hermite polynomials. Comparison of Cox & Munk's experimental data with the Gram-Charlier distribution indicates that the probability distribution for the cross-wind direction is very close to the Gaussian distribution, whereas for the up-wind direction, some skewness is observed.

Let us now present the sea surface ordinates in the form of the Fourier-Stjeltjes integral (Massel 1996):

$$\zeta(x, y, t) = \int_{-\infty}^{\infty}\int_{-\pi}^{\pi} \exp[ik(x\cos\Theta + y\sin\Theta) - i\omega t]\, dA(\omega, \Theta), \tag{41}$$

where Θ is the direction of a particular wave spectral component.

The spectral amplitude $A(\omega, \Theta)$ is related to the two-dimensional frequency-directional spectrum $S_1(\omega, \Theta)$ as follows:

$$\overline{dA(\omega,\Theta)\, dA^*(\omega', \Theta')} = S_1(\omega,\Theta)\delta(\omega - \omega')\delta(\Theta - \Theta')\, d\omega\, d\omega'\, d\Theta\, d\Theta', \tag{42}$$

in which $\delta(\,)$ is Dirac's delta and $(*)$ denotes the complex conjugate value.

Therefore, the surface slope components along the up-wind and cross-wind directions now become

$$\varepsilon_u = \frac{\partial \zeta}{\partial x} = \int_{-\infty}^{\infty} \int_{-\pi}^{\pi} (ik\cos\Theta) \exp[ikx\cos\Theta + y\sin\Theta) - i\omega t]\, dA(\omega, \Theta) \quad (43)$$

and

$$\varepsilon_c = \frac{\partial \zeta}{\partial y} = \int_{-\infty}^{\infty} \int_{-\pi}^{\pi} (ik\sin\Theta) \exp[ikx\cos\Theta + y\sin\Theta) - i\omega t]\, dA(\omega, \Theta). \quad (44)$$

Using eq. (32) and the known relation

$$\int_{-\infty}^{\infty} \delta(x-y)\, dx = f(y), \quad (45)$$

we obtain

$$\left.\begin{aligned} \sigma_u^2 &= \int_{-\infty}^{\infty} \int_{-\pi}^{\pi} k^2 \cos^2\Theta\, S_1(\omega,\Theta)\, d\omega\, d\Theta \\ \sigma_c^2 &= \int_{-\infty}^{\infty} \int_{-\pi}^{\pi} k^2 \sin^2\Theta\, S_1(\omega,\Theta)\, d\omega\, d\Theta \end{aligned}\right\}. \quad (46)$$

If we restrict our attention to deep waters, when the dispersion relation is $\omega^2 = gk$, the mean square slopes are

$$\left.\begin{aligned} \sigma_u^2 &= \int_{-\infty}^{\infty} \int_{-\pi}^{\pi} \frac{\omega^4}{g^2} \cos^2\Theta\, S_1(\omega,\Theta)\, d\omega\, d\Theta \\ \sigma_c^2 &= \int_{-\infty}^{\infty} \int_{-\pi}^{\pi} \frac{\omega^4}{g^2} \sin^2\Theta\, S_1(\omega,\Theta)\, d\omega\, d\Theta \end{aligned}\right\}. \quad (47)$$

4.2. Influence of directional spreading on surface wave slopes

The governing equations in Section 4.1 indicate that the probability density of the surface slopes $f(\varepsilon, \theta_1)$ and the mean square slopes σ_u^2 and σ_c^2 are strongly dependent on the specific form of the directional spreading function $D(\Theta, \omega)$. In this Section we examine various types of directional spreading and the resulting mean square slopes.

4.2.1. Unimodal spreading as a function of direction only

In the simplest case we assume that the two-dimensional wave spectrum $S_1(\omega, \Theta)$ takes the form

$$S_1(\omega, \Theta) = S(\omega) D(\Theta). \quad (48)$$

After substituting eq. (48) in eq. (47) we obtain

$$\left.\begin{aligned} \sigma_u^2 &= \frac{1}{g^2}\int_{-\infty}^{\infty}\omega^4\,S(\omega)d\omega\int_{-\pi}^{\pi}\cos^2\Theta D(\Theta)\,d\Theta \\ \sigma_c^2 &= \frac{1}{g^2}\int_{-\infty}^{\infty}\omega^4\,S(\omega)\,d\omega\int_{-\pi}^{\pi}\sin^2\Theta\,D(\Theta)\,d\Theta \end{aligned}\right\}. \tag{49}$$

Taking into account the fact that the integral against the frequency is simply the fourth spectral moment, we can rewrite eq. (49) in the form

$$\left.\begin{aligned} \sigma_u^2 &= \frac{m_4}{g^2}\int_{-\pi}^{\pi}\cos^2\Theta D(\Theta)\,d\Theta = \frac{m_4}{g^2}I_u \\ \sigma_c^2 &= \frac{m_4}{g^2}\int_{-\pi}^{\pi}\sin^2\Theta\,D(\Theta)\,d\Theta = \frac{m_4}{g^2}I_c \end{aligned}\right\}, \tag{50}$$

where

$$m_4 = \int_{-\infty}^{\infty}\omega^4\,S_1(\omega)\,d\omega \tag{51}$$

and

$$I_u = \int_{-\pi}^{\pi}\cos^2\Theta D(\Theta)\,d\Theta \qquad \text{and} \qquad I_c = \int_{-\pi}^{\pi}\sin^2\Theta D(\Theta)\,d\Theta. \tag{52}$$

Equation (50) indicates that the mean-square slope depends on the product of the frequency distribution of the wave energy (spectral moment m_4) and on the function of directional spreading $D(\Theta)$. The mean square of the total slope (regardless of direction) now becomes

$$\sigma_u^2 + \sigma_c^2 = \frac{m_4}{g^2}\int_{-\pi}^{\pi}D(\Theta)\,d\Theta = \frac{m_4}{g^2}. \tag{53}$$

The two-dimensional probability function of the surface slope and direction can be obtained by substituting eq. (50) in eq. (34):

$$f(\varepsilon,\theta_1) = \frac{\varepsilon}{2\pi\tilde{m}_4\sqrt{I_u\,I_c}}\exp\left\{-\frac{\varepsilon^2}{\tilde{m}_4}\,\frac{I_c\cos^2\theta_1 + I_u\sin^2\theta_1}{2I_u\,I_c}\right\}, \tag{54}$$

where

$$\tilde{m}_4 = \frac{m_4}{g^2}. \tag{55}$$

Integration of eq. (54) against θ_1, results in the probability density function for surface slopes, regardless of the direction θ_1, as follows:

$$f(\varepsilon) = \frac{\varepsilon}{\tilde{m}_4\sqrt{I_u\, I_c}} \exp\left[-\frac{\varepsilon^2}{4\tilde{m}_4 I_u\, I_c}\right]\, I_0\left[\frac{\varepsilon^2(I_u - I_c)}{4\tilde{m}_4 I_u\, I_c}\right], \tag{56}$$

in which $I_0(x)$ is the modified zero-order Bessel function (Abramowitz & Stegun 1975).

Let us make the following variable transformation in eq. (56):

$$\xi = \frac{\varepsilon}{(\tilde{m}_4)^{1/2}}. \tag{57}$$

After substituting the above relation we obtain

$$f(\xi) = \frac{\xi}{\sqrt{I_u I_c}} \exp\left[-\frac{\xi^2}{4I_u I_c}\right]\, I_0\left[\frac{\xi^2}{4}\,\frac{I_u - I_c}{I_u I_c}\right]. \tag{58}$$

This probability density function will be used to examine some special cases of directional spreading.

In particular, when the wave energy is uniformly distributed in all directions, the directional spreading takes the form

$$D(\Theta) = \frac{1}{2\pi}. \tag{59}$$

Then the probability density function (eq. (54)) becomes

$$f(\varepsilon, \theta_1) = \frac{\varepsilon}{\pi\,\tilde{m}_4} \exp\left(-\frac{\varepsilon^2}{\tilde{m}_4}\right), \tag{60}$$

and after integration against angle θ_1 we have

$$f(\varepsilon) = 2\frac{\varepsilon}{\tilde{m}_4} \exp\left(-\frac{\varepsilon^2}{\tilde{m}_4}\right). \tag{61}$$

Therefore, for short-crested and uniformly distributed waves, the surface slope distribution is the Rayleigh distribution, which, contrary to expectation, does not depend on the direction θ_1. The ratio of the mean square slopes σ_u^2 and σ_c^2 is

$$\frac{\sigma_c^2}{\sigma_u^2} = \frac{I_c}{I_u} = 1. \tag{62}$$

On the other hand, it can be shown that for very narrow directional spreading, when all spectral wave components propagate along the x axis, the directional spreading is simply

$$D(\Theta) = \delta(\Theta - \Theta_0), \tag{63}$$

where $\Theta_0 = 0$, and the probability density function (eq. (58)) becomes

$$f(\xi) = \sqrt{\frac{2}{\pi}} \exp\left(-\frac{1}{2}\,\xi^2\right). \tag{64}$$

The above equation indicates that when wave crests are very long (a very narrow directional distribution), surface slopes are normally distributed (truncated normal distribution).

The directional spreading function frequently used in practice has the form as in eq. (20). For very narrow directional spreading ($s \geq 10$), the integrals in eq. (52) become $I_u \to 1$ and $I_c \to 0$. Thus, almost all the wave energy propagates along the wind direction, whereas the amount of energy in the cross-wind direction is very small. Therefore, $I_c/I_u \to 0$. On the other hand, for small values of the directionality parameter s, both integrals I_u and I_c are almost the same, i.e. $\lim\limits_{s\to 0} (I_c/I_u) = 1$, and the wave energy becomes uniformly distributed in all directions.

The mean square slopes σ_u^2 and σ_c^2 follow from eq. (50). Therefore we have

$$\left.\begin{aligned} \sigma_u^2 &= 0.076 a_4 \left(\frac{gX}{U^2}\right)^{-0.22} I_u \\ \sigma_c^2 &= 0.076 a_4 \left(\frac{gX}{U^2}\right)^{-0.22} I_c \end{aligned}\right\}, \tag{65}$$

where coefficient a_4 is given in eq. (19).

The above equations indicate that the ratio of the mean square slopes σ_c^2/σ_u^2 does not depend on the frequency characteristics of the wave field and is a function of the directional spreading only. Table 1 shows the ratio of the mean square slopes for selected values of the directionality parameter s. It should be noted that the observed cross-wind component of the mean square slope can be very high and for some s values even equal to the up-wind component.

To define the relationship between the mean-square-slopes and the wind speed U_{10} and wind fetch X we again use Cox & Munk's (1954) data. In this experiment, however, the exact values of the wind fetches are not known. Thus in Figure 2, the up-wind mean-square slope is shown for three specified wind fetches, i.e. $X = 10$, 50 and 100 km and directional spreading

Table 1. Ratio of the mean square slopes for directionality parameter $s = 1, 2, 3$

s	directional spreading	I_u	I_c	σ_c^2/σ_u^2
1	$\sim \cos^2\theta$	0.50	0.50	1.00
2	$\sim \cos^4\theta$	0.58	0.42	0.72
3	$\sim \cos^6\theta$	0.65	0.35	0.54

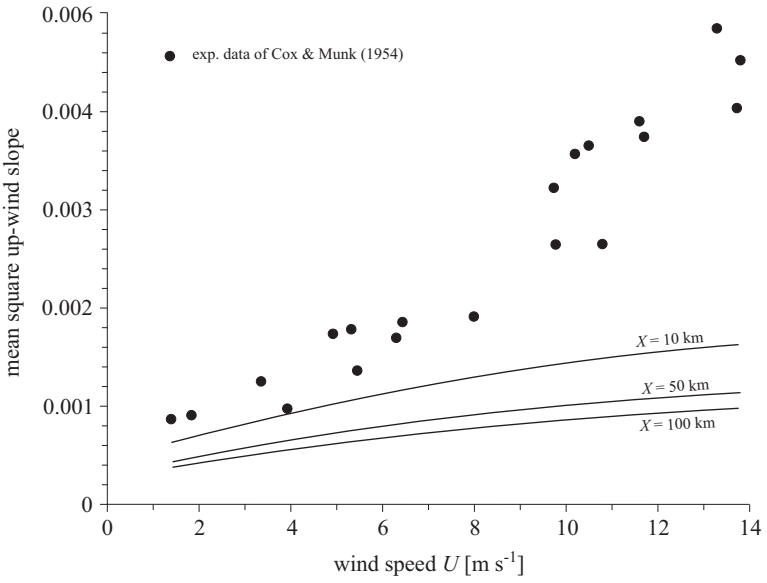

Figure 2. Up-wind mean square slope as a function of wind speed. Comparison of theoretical unimodal spreading with Cox & Munk's (1954) data

$\cos^2(\Theta)$. From the figure it follows that the theoretical values of the mean square slopes due to unimodal directional spreading are smaller than the experimental ones given by Cox & Munk (1954), especially for stronger winds. The same conclusion is also valid for the cross-wind slopes.

More general information on the sea surface slopes is provided by the probability density function. In particular, it will be interesting to compare this function for two specific directions, for example, for $\theta_1 = 0$ (up-wind direction) and for $\theta_1 = 90^\circ$ (cross-wind direction). Therefore, from eq. (54) we have

$$f(\varepsilon, 0^\circ) = \frac{\varepsilon}{2\pi \dfrac{m_4}{gz}} \sqrt{I_u I_c} \exp\left[-\frac{\varepsilon^2}{\dfrac{2m_4}{gz} I_u} \right], \tag{66}$$

or

$$f(\varepsilon, 0^\circ) = \frac{\varepsilon}{2\pi\,\sigma_u\sigma_c}\,\exp\left[-\frac{\varepsilon^2}{2\sigma_u^2}\right]. \tag{67}$$

Similarly, for the cross-wind direction we obtain

$$f(\varepsilon, 90^\circ) = \frac{\varepsilon}{2\pi\,\sigma_u\sigma_c}\,\exp\left[-\frac{\varepsilon^2}{2\sigma_c^2}\right]. \tag{68}$$

Equations (67) and (68) are illustrated in Figure 3 for one case from Cox & Munk's (1954) experiments, when $U = 10.2\,\mathrm{m\,s^{-1}}$ and $\sigma_u^2 = 0.0357$, $\sigma_c^2 = 0.0254$. Both probability density functions exhibit the Rayleigh distribution form. The most probable slopes in the up- and cross-wind directions correspond to the slope $\varepsilon \sim 0.2$. Note that functions (67) and (68) are the probability density functions of the modules of slopes observed in the particular directions. They should not be confused with the probability density functions for the up- and cross-wind components or with the projection of the two-dimensional probability density function onto the up- and cross-wind directions, as given by Cox & Munk (1954) – see also the discussion in Section 4.1.

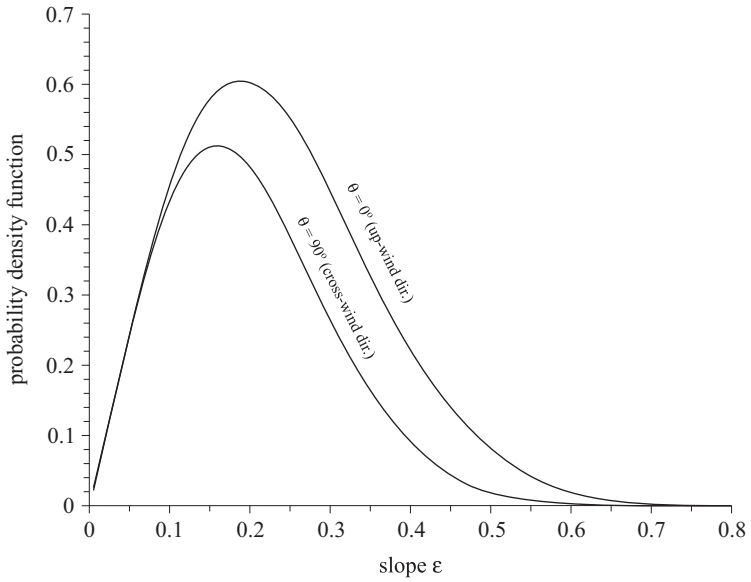

Figure 3. Probability density function of slopes in specific directions

4.2.2. Bimodal directional spreading function

Let us now examine the applicability of bimodal directional spreading (eq. (27)) to the representation of mean square slopes. After substituting the JONSWAP frequency spectrum (eq. (12)) and bimodal representation (eq. (27)) in function (47), we obtain

$$\begin{Bmatrix} \sigma_u^2 \\ \sigma_c^2 \end{Bmatrix} = \alpha \int_{0.5}^{\omega_u/\omega_p} \hat{\omega}^{-1} \exp\left(-\frac{5}{4}\hat{\omega}^{-4}\right) \gamma^{\delta(\hat{\omega})} \int_{-180^\circ}^{180^\circ} \begin{Bmatrix} \cos^2\theta \\ \sin^2\theta \end{Bmatrix} D(\theta;\hat{\omega}) d\theta \, d\hat{\omega}, \tag{69}$$

where $\hat{\omega} = \omega/\omega_p$.

The bimodal function (eq. (27)) suggested by Ewans (1998) does not depend on the wave component frequency but on the ratio $\hat{\omega} = \omega/\omega_p$. The integrals in the above equations are therefore constants. The only dependence on wind speed U and wind fetch X is due to parameter α (see eq. (15)). Hence, from eq. (69) we have

$$\left.\begin{aligned} \sigma_u^2 &= 0.9680\alpha \\ \sigma_c^2 &= 0.7375\,\alpha \\ \sigma_c^2/\sigma_u^2 &= 0.7619 \end{aligned}\right\}. \tag{70}$$

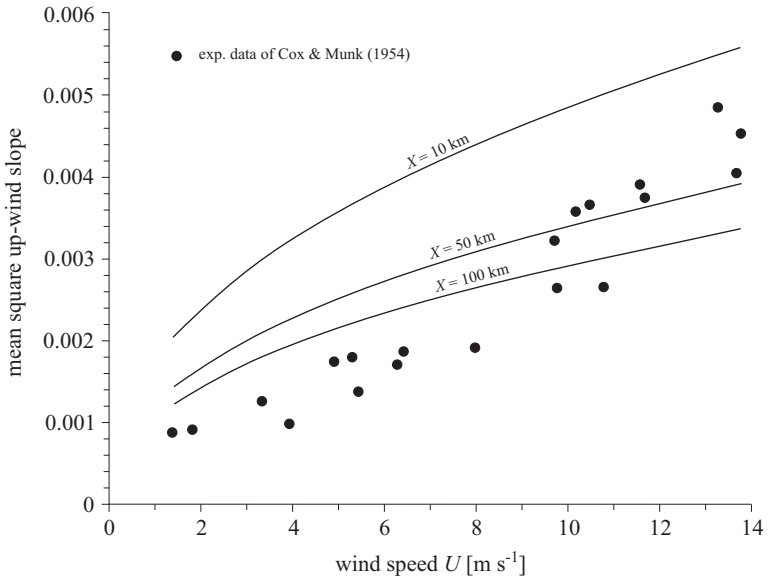

Figure 4. Up-wind mean square slope as a function of wind speed. Comparison of theoretical bimodal spreading with Cox & Munk's (1954) data

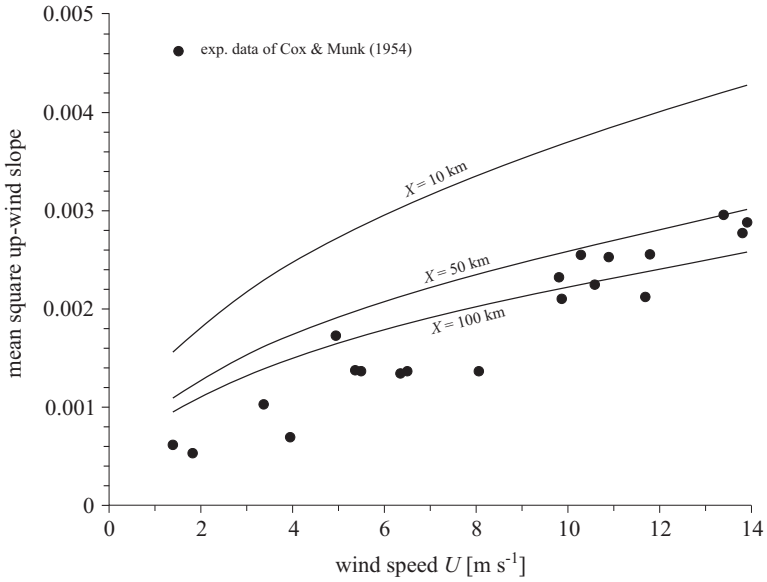

Figure 5. Cross-wind mean square slope as a function of wind speed. Comparison of theoretical bimodal spreading with Cox & Munk's (1954) data

The theoretical formulae (69) are compared with Cox & Munk's experimental data in Figures 4 and 5 for selected wind fetches $X =$ 10, 50, 100 km. The agreement is now much better than in the case of the unimodal directional spreading, especially for wind fetch $X =$ 100 km.

Comparison with Pelevin & Burtsev's (1975) experimental data, which contains information on wind speed U and wind fetch X, shows that data with a higher value of $\alpha = 0.076(gX/U^2)^{-0.22}$ (low wind speed) are much closer to the theoretical line than data corresponding to the smaller value of α (high wind speed). In both cases, however, the discrepancy between theory and experiment is bigger than in the case of Cox & Munk's data.

5. Surface area of an ocean wave

The area of a wind-roughened sea surface is an important parameter for estimating the mass and momentum fluxes to and from the oceans. It is evident that the area of a wind-roughened sea surface is larger that of a calm sea. The increase in the area of sea surface depends on the geometry of the surface waves. In order to estimate this increase in sea area we first discuss regular surface waves.

5.1. Regular waves

Let us consider the ocean surface (without waves) in the form of a rectangle with dimensions a and b, where a lies parallel to the x axis and b is parallel to the y axis. The area of the surface is therefore $S_0 = a \times b$. How will the area of this sea surface change when a regular wave of height H and length L propagates in the direction of the x axis? As the crest of a regular wave is parallel to the y axis, the sea surface elevation for a given time $t = 0$ is

$$\zeta(x) = \frac{H}{2} \cos\left(\frac{2\pi x}{L}\right). \tag{71}$$

The area of a wind-roughened surface can therefore be given by

$$S = l\, b, \tag{72}$$

in which l is the length of the arc of the wave profile, when we intersect the sea surface by a vertical plane parallel to the x axis within the limits from $x = 0$ to $x = a$. The length arc l becomes (Abramowitz & Stegun 1975)

$$l = \int_0^a \sqrt{1 + \left(\frac{\partial \zeta(x)}{\partial x}\right)^2}\, dx. \tag{73}$$

After substituting eq. (73) in eq. (72) we get

$$S = \frac{Lb}{2\pi} \int_0^{ka} \sqrt{1 + \left(\frac{kH}{2}\right)^2 \sin^2(u)}\, du, \tag{74}$$

in which k is the wave number $k = 2\pi/L$.

The exact solution of equation (74) is expressed in the form of an elliptic integral of the second kind (Abramowitz & Stegun 1975), which cannot be obtained analytically. However, as the quantity $kH/2 = \pi H/L$ is usually very small, we can expand the function under the integral into a Taylor series as follows:

$$\sqrt{1 + \left(\frac{kH}{2}\right)^2 \sin^2 u} \approx 1 + \frac{1}{2}\left(\frac{kH}{2}\right)^2 \sin^2(u) - \frac{1}{8}\left(\frac{kH}{2}\right)^4 \sin^4(u) + \cdots \tag{75}$$

As we are dealing with regular waves, we can restrict ourselves to one wave length and thus take $a = L$ ($ka = 2\pi$). Using this in eq. (74), we obtain

$$S = Lb\left[1 + \frac{1}{4}\left(\frac{kH}{2}\right)^2 - \frac{3}{64}\left(\frac{kH}{2}\right)^4 + \cdots\right]. \tag{76}$$

Therefore, the relative increase in the sea surface area becomes

$$\delta = (S - S_0)/S_0 = \left[\frac{1}{4}\left(\frac{kH}{2}\right)^2 - \frac{3}{64}\left(\frac{kH}{2}\right)^4 + \cdots\right]. \tag{77}$$

The relative increase in sea surface area $\delta = (S - S_0)/S_0$ (in %) as a function of wave steepness H/L is illustrated in Figure 6.

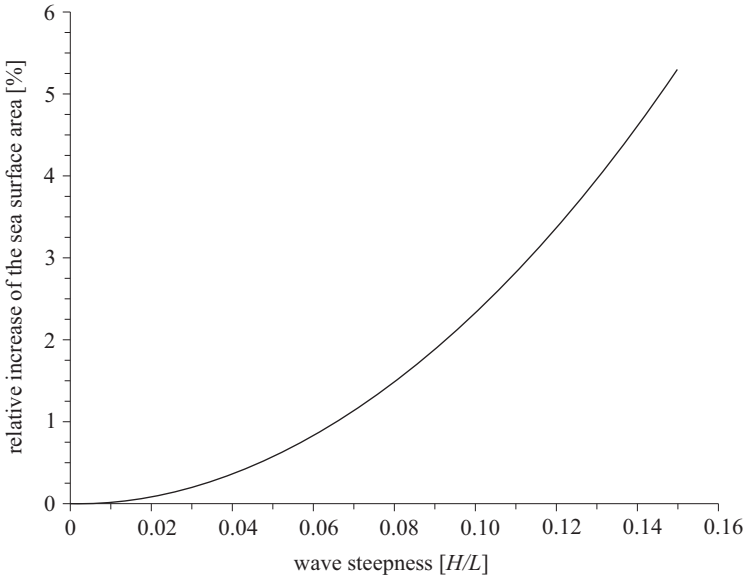

Figure 6. Relative increase of the sea surface area as a function of wave steepness for one regular wave

Let us now assume that two regular surface waves of heights H_1 and H_2, and lengths L_1 and L_2 are propagating in two different directions θ_1 and θ_2. The resulting surface elevation takes the form

$$\begin{aligned}\zeta(x,y,t) &= \frac{H_1}{2}\cos\left[\frac{2\pi}{L_1}(x\cos\theta_1 + y\sin\theta_1) - \omega_1 t\right] + \\ &+ \frac{H_2}{2}\cos\left[\frac{2\pi}{L_2}(x\cos\theta_2 + y\sin\theta_2) - \omega_2 t\right],\end{aligned} \tag{78}$$

and the area of wave surface is now (Abramowitz & Stegun 1975)

$$S = \int_0^a \int_0^b \sqrt{1 + \left(\frac{\partial\zeta}{\partial x}\right)^2 + \left(\frac{\partial\zeta}{\partial y}\right)^2}\, dy\, dx, \tag{79}$$

in which a and b are the dimensions of a sea surface area without waves.

Figure 7 presents the relative increase in sea surface area $\delta = (S - S_0)/S_0$ as a function of the angle propagation difference $(\theta_1 - \theta_2)$ for short waves $(H_1 = H_2 = 1\,\mathrm{m},\ T_1 = T_2 = 4\ \mathrm{s})$. The maximum increase in sea area (about 6%) is observed for waves propagating in the same or in opposite directions. For other angles, the δ value is about 3%.

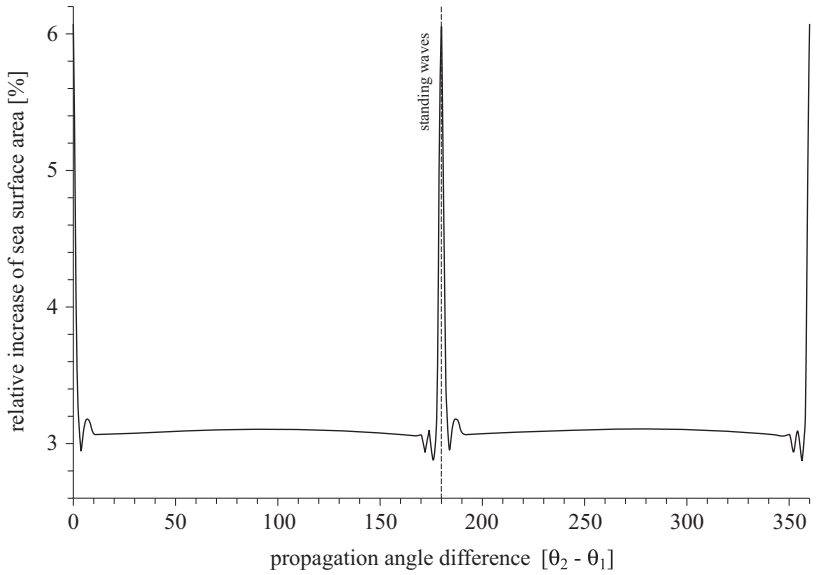

Figure 7. Relative increase of the sea surface area as a function of wave directions for two intersecting regular short waves

For two long waves the relative increase is much smaller than in the case of shorter waves as the sea surface is smoother. In the same way we can calculate the area of the sea surface consisting of an arbitrary number of intersecting regular waves.

5.2. Wind-induced waves

Under natural conditions, wave profiles are constantly changing with time in random fashion. Owing to the complex energy transfer from the atmosphere to the ocean and vice versa, the resulting surface waves are multidirectional.

Information about a time series of surface displacements at a given point is usually available from a wave recorder or from numerical simulation. For the purpose of this paper we use the simulation approach and assume that a confused sea is the summation of many independent harmonics travelling

in various directions. These harmonics are superimposed with a random phase φ, which is uniformly distributed on $(-\pi, \pi)$. Thus we have (Massel & Brinkman 1998)

$$\zeta(x, y, t) = \sum_{m=1}^{M_1} \sum_{n=1}^{N_1} a_{mn} \cos[k_m x \cos\theta_n + k_m y \sin\theta_n - \omega_m t + \varphi_{mn}], \quad (80)$$

in which the deterministic amplitudes a_{mn} are prescribed by the following formula:

$$a_{mn}^2 = 2S_1(\omega, \theta)\Delta\omega_m \Delta\omega_n, \quad (81)$$

where $S_1(\omega, \theta)$ is the input frequency-directional spectrum, $\Delta\omega_m$ denotes the band-width of the mth frequency, and $\Delta\omega_n$ is the band-width of the nth wave angle. The wave numbers k_m are given by the dispersion relation

$$\omega_m^2 = g k_m \tanh(k_m h) \quad (82)$$

and M_1 and N_1 are the respective numbers of frequencies and directions used in the simulation.

We represent the input frequency-directional spectrum $S_1(\omega, \theta)$ in the form of the product of the frequency spectrum $S_1(\omega)$ and the directional spreading $D(\theta)$, in which the JONSWAP frequency spectrum (eq. (12)) is

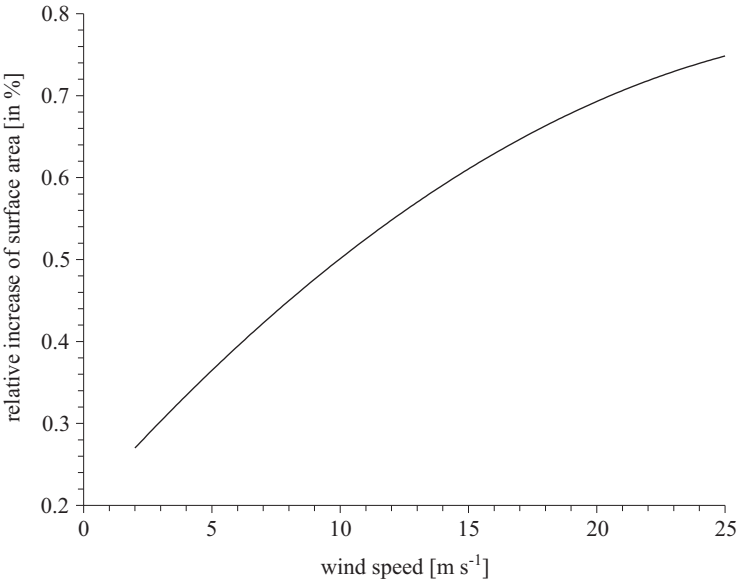

Figure 8. Relative increase of the irregular sea surface area as a function of wind speed

used, and for the directional spreading function $D(\theta)$ we adapt formula (20) with parameter $s = 1$.

To simulate the sea surface, a time series of $M_1 = 155$ frequencies non-uniformly distributed in the frequency band $0.5\,\omega_p < \omega < 6\,\omega_p$ and $N_1 = 180$ directions ($\Delta\theta = 2^\circ$) were used. When the surface displacement $\zeta = \zeta(x, y, t)$ is known, the area of random sea surface over the plain rectangle $a \times b$ is given by eq. (79).

Let us assume that an area of 1 km $\times$ 1 km is covered by surface waves induced by a wind of velocity changing from $U = 2$m/s to $U = 25$m/s and fetch $X = 100$ km. The relationship between the relative increase in area δ and wind speed U is shown in Figure 8. In a very severe storm, when $U = 25$ m s^{-1} and significant wave height $H_s = 4.57$ m, the increase δ approaches the value of $\delta = 0.77\%$.

6. Conclusions

This paper examines some geometrical features of ocean surface waves, which are of special importance in air-sea interaction and incipient wave breaking. In particular, the paper demonstrates the influence of directional spreading on the statistics of sea surface slopes. Theoretical analysis and comparison with the available experimental data show that unimodal directional spreading is unable to reproduce properly the observed ratio of the cross-wind/up-wind mean square slopes. Better agreement is achieved when bimodal directional spreading, consisting of two wrapped-Gaussian distributions, is applied. The form of spreading suggested by Ewans is used in the paper. Besides the progress made with bidirectional spreading, the accurate reproduction of sea surface slopes still requires more study. The second part of the paper discusses the increase in the sea surface area as a result of wave motion. The formulae developed show that the increase in area is in fact rather small for both regular and irregular surface waves.

References

Abramowitz M., Stegun I. A., 1975, *Handbook of mathematical functions*, Dover Publ., New York, 1045 pp.

Apel J. R., 1994, *An improved model of the ocean surface wave vector spectrum and its effects on radar backscatter*, J. Geophys. Res., 99 (C8), 16 269–16 291.

Banner M. L., 1990, *Equilibrium spectra of wind waves*, J. Phys. Oceanogr., 20 (7), 966–984.

Banner M. L., Young I. R., 1994, *Modelling spectral dissipation in the evolution of wind waves. Part I: Assessment of existing model performance*, J. Phys. Oceanogr., 24 (7), 1550–1571.

Bjerkas A. W., Riedel F. W., 1979, *Proposed model for the elevation spectrum of a wind-roughened sea surface*, Tech. Rep., APL-TG-1328-I-31, Appl. Phys. Lab., Johns Hopkins Univ., 31 pp.

Cox C., Munk W., 1954, *Measurement of the roughness of the sea surface from photographs of the sun's glitter*, J. Opt. Soc. Am., 44 (11), 838–850.

Donelan M. A., Hamilton J., Hui W. H., 1985, *Directional spectra of wind-generated waves*, Philos. T. Roy. Soc. A, 315 (1534), 509–562.

Elfouhaily T., Chapron B., Katsaros K., 1997, *A unified directional spectrum for long and short wind-driven waves*, J. Geophys. Res., 102 (C7), 15 781–15 796.

Ewans K. C., 1998, *Observations of the directional spectrum of fetch-limited waves*, J. Phys. Oceanogr., 28 (3), 495–512.

Ewans K. C., van der Vlugt T., 1999, *Estimating bimodal frequency-direction spectra from surface buoy data recorded during tropical cyclones*, J. Offshore Mech. Arct., 121 (3), 172–180.

Goda Y., 1981, *Simulation in examination of directional resolution*, [in:] *Directional wave spectra*, R. L. Wiegel (ed.), ASCE, Waterway, 387–407.

Hasselmann K., Barnett T. P., Bouws E., Carlson H., Cartwright D. E., Enke K., Ewing J. A., Gienapp H., Hasselmann D. E., Kruseman P., Meerburg A., Müller P., Olbers D. J., Richter K., Sell W., Walden H., 1973, *Measurements of wind-wave growth and swell decay during the Joint North Sea Wave Project (JONSWAP)*, Deutsches Hydr. Zeit., A 12, 1–95.

Hasselmann D. E., Dunckel M., Ewing J. A., 1980, *Directional wave spectra observed during JONSWAP 1973*, J. Phys. Oceanogr., 10 (8), 1264–1280.

Heron M. L., Skirving W. J., Michael K. J., 2006, *Short-wave ocean wave slope models for use in remote sensing data analysis*, IEEE T. Geosci. Remote, 44 (7), 1962–1973.

Hughes B. A., Grant H. L., Chappell R. W., 1977, *A fast response surface-wave slope meter and measured wind-wave moments*, Deep-Sea Res., 24 (12), 1211–1223.

Hwang P. A., Shemdin O. H., 1988, *The dependence of sea surface slope on atmospheric stability and swell conditions*, J. Geophys. Res., 93 (C11), 13 903–13 912.

Hwang P. A., Wang D. W., 2001, *Directional distributions and mean square slopes in the equilibrium and saturation ranges of the wave spectrum*, J. Phys. Oceanogr., 31 (5), 1346–1360.

Krylov J. M., Strekalov S. S., Cyplukhin V. F., 1976, *Wind waves and their effect on marine constructions*, Gidrometeoizdat, Leningrad, 256 pp., (in Russian).

Kuik A. J., van Vledder Ph., Holthuijsen L. H., 1988, *A method for the routine analysis of pitch-and-roll buoy wave data*, J. Phys. Oceanogr., 18 (7), 1020–1034.

Longuet-Higgins M. S., 1957, *The statistical analysis of a random, moving surface*, Phil. T. Roy. Soc., 249 (966), 321–387.

Longuet-Higgins M. S., Cartwright D. E., Smith N. D., 1961, *Observations of the directional spectrum of sea waves using the motions of a floating buoy*, [in:] *Ocean wave spectrum*, Prentice-Hall Inc., Engelwood Cliffs, 111–136.

Mardia K. V., 1972, *Statistics of directional data*, Acad. Press, London, 240 pp.

Massel S. R., 1996, *Ocean surface waves: their physics and prediction*, World Sci. Publ., Singapore, 491 pp.

Massel S. R., 2007, *Ocean waves breaking and marine aerosol fluxes*, Springer, New York, 323 pp.

Massel S. R., Brinkman R. M., 1998, *On the determination of directional wave spectra for practical applications*, Appl. Ocean Res., 20 (6), 357–374.

Mitsujasu H., Suhaya T., Mizuno S., Ohkuso M., Honda T., Rikiishi K., 1975, *Observations of the directional spectrum of ocean waves using a cloverleaf buoy*, J. Phys. Oceanogr., 5 (4), 750–760.

Pelevin V. N., Burtsev J. G., 1975, *The measurements of the sea surface slope distribution under the wind roughness*, [in:] *Optical investigations in the ocean and in the atmosphere above the ocean*, Inst. Okean. AN SSSR, 202–218, (in Russian).

Wang D. W., Hwang P. A., 2001, *Evolution of the biomodal directional distribution of ocean waves*, J. Phys. Oceanogr., 31 (5), 1200–1221.

Woźniak S. B., 1996, *Sea surface slope distribution and foam coverage as functions of the mean height of wind waves*, Oceanologia, 38 (3), 317–332.

Young I. R., Verhagen L. A., Banner M. L., 1995, *A note on the bimodal directional spreading of fetch-limited wind waves*, J. Geophys. Res., 100 (C1), 773–778.